Sanjou, Michio; Nezu, Iehisa; Okamoto, Taka-aki

Effect of Submergence Depth on Turbulence Structure in Vegetated Canopy Open-Channel Flows

EFFECT OF SUBMERGENCE DEPTH ON TURBULENCE STRUCTURE IN VEGETATED CANOPY OPEN-CHANNEL FLOWS

Michio Sanjou [1], Iehisa Nezu [2], and Taka-aki Okamoto [3]

[1] Assistant Professor, Department of Civil Engineering, Kyoto University
Katsura Campus, Kyoto 615-8540, Japan, e-mail: sanjou@mbox.kudpc.kyoto-u.ac.jp
[2] Professor, Department of Civil Engineering, Kyoto University
Katsura Campus, Kyoto 615-8540, Japan, e-mail: Iehisa.Nezu@mbox.kudpc.kyoto-u.ac.jp
[3] Ph. D student, Department of Civil Engineering, Kyoto University
Katsura Campus, Kyoto 615-8540, Japan, e-mail: takaakiokamoto@t02.mbox.media.kyoto-u.ac.jp

ABSTRACT

It is very important in river environment and hydraulic engineering to study the hydrodynamics of vegetated canopy open-channel flows. The velocity profiles within canopy layer are varied largely in the vertical direction due to the drag effect of vegetation. The momentum and energy are transported to turbulence from mean flow, and consequently, coherent organized motion is generated due to the K-H instability. In these vegetated flows, the submergence depth, i.e., the ratio of the water depth to the vegetation height, may dominate the turbulence structure significantly. In order to reveal such an effect of submergence depth, PIV measurements were conducted in vegetated open-channel flows by changing the submergence depth in a wide range. As the results, mean-flow properties, turbulence structure and coherent motions were revealed and discussed in detail.

Keywords: vegetated canopy, submergence depth, coherent eddy and PIV measurements

1. INTRODUCTION

A large amount of aquatic plants in actual rivers influence the mean-flow property and turbulence structure significantly. In submerged canopy open-channel flows, an additional drag force due to vegetation reduces the time-averaged mean velocity within the canopy. The velocity difference at the tip of canopies produces a strong shear layer, which generates coherent eddies and organized motion, e.g., sweeps and ejections. As these coherent motions have significant relation with an enhancement of mass and momentum exchanges between the vegetated and the non-vegetated zones, a lot of researchers these have studied these topics intensively.

As an earlier study, Raupach &Thom (1986) have measured turbulence structure within plant model canopies by using hot-wire anemometers. They found that the turbulent diffusion in the turbulent energy budget is a major energy loss near the top of the canopy and that the wake production is greater than the shear production within the plant layer. Dwyer *et al.*(2004) have calculated the turbulence kinetic energy (TKE) budget by using a large eddy simulation (LES) and showed the relation between the vegetation elements and the energy transport. Nepf & Vivoni (2000) have conducted ADV measurements in vegetated open-channel flows by changing the submergence depth H/h, and compared the submerged vegetated flow with the emergent one. They classified the within-canopy layer into two regions. One is the lower canopy layer, called the 'longitudinal exchange zone' and the other is the upper canopy layer, called the 'vertical exchange zone'. Poggi et al.(2004) have measured the vegetated open-channel flow by a laser Doppler anemometer (LDA). They classified the whole flow-depth region into three layers. The lower layer is dominated by vortices due to Karman vortex. The second layer is, which is near the canopy top, which is dominated by K-H waves due to inflection instability, and the third is the upper layer which is similar to boundary layers. Wilson et al. (2003) have examined two kinds of flexible vegetation on the effects of turbulence structures. The attachment of the plant foliage on the top of the stems reduced the turbulent mixing between the within-canopy layer and the over-canopy layer. Nezu et al. (2006) conducted turbulence measurements in vegetated open-channel flow by using two-component LDA and revealed the effects of vegetation density on turbulence structures.

However, the instantaneous coherent structures are not available. In the present study, PIV measurements in vegetated open-channel flows in order to investigate the relation between the submergence depth and coherent structure. The generation source, length-scale and periodicity of coherent eddies were examined.

Table.1 Hydraulic condition

	U_m (cm/s)	H (cm)	h (cm)	Re	Fr	a(1/m)
Case1		4.5		4500	0.15	
Case2		6.25		6250	0.13	
Case3		7.5		7500	0.12	
Case4	10.0	10.0	5.0	10000	0.10	7.6
Case5		12.5		12500	0.09	
Case6		15.0		15000	0.08	
Case7		20.0		20000	0.07	

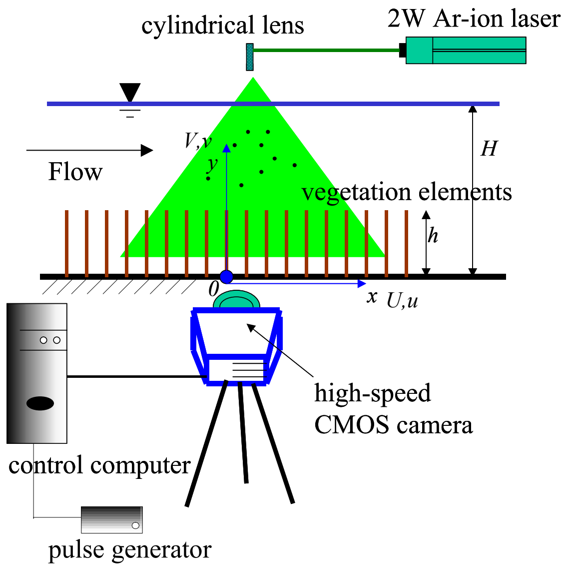

Fig.1 Experimental set-up

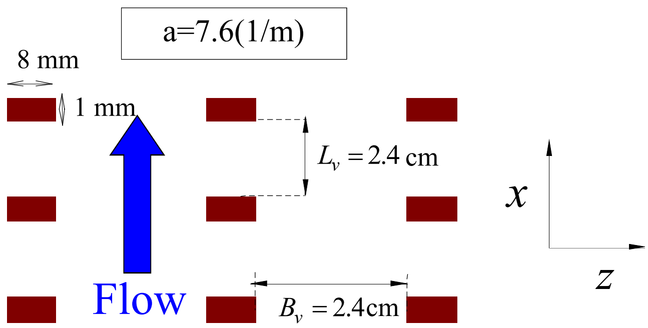

Fig.2 Allocation pattern of vegetation (top view)

2. EXPERIMENTAL METHOD

Fig.1 shows the experimental setup and the coordinate system. The experiments were conducted in a 10m long and 40cm wide glass-made flume. The elements of vegetation model were composed of non-flexible strip plates. These vegetation elements were attached vertically on the flume bed. The size of this element is h=50mm height, 8mm width and 1mm thickness. H is the water depth and h is the vegetation height. B_v=2.4cm and L_v=2.4cm are the neighbouring vegetation spacings in the spanwise and streamwise directions, respectively, as shown in Fig.2. That is to say, the allocation of vegetation is a square pattern of 24mm×24mm x, y and z are the streamwise, vertical and spanwise coordinates. The vertical origin, $y = 0$, is chosen as the channel bed. The time-averaged velocity components in each direction are defined as U, V and W, and the turbulent fluctuations are u, v and w, respectively.

In order to measure two-component instantaneous velocities, i.e., $\tilde{u}(t) \equiv U + u(t)$ and $\tilde{v}(t) \equiv V + v(t)$, within and above the canopy, a laser light sheet (LLS) was projected into the water column vertically from the free surface. The 2mm thick LLS was generated by 2W Argon-ion laser using a cylindrical lens. The illumination position of LLS were located at

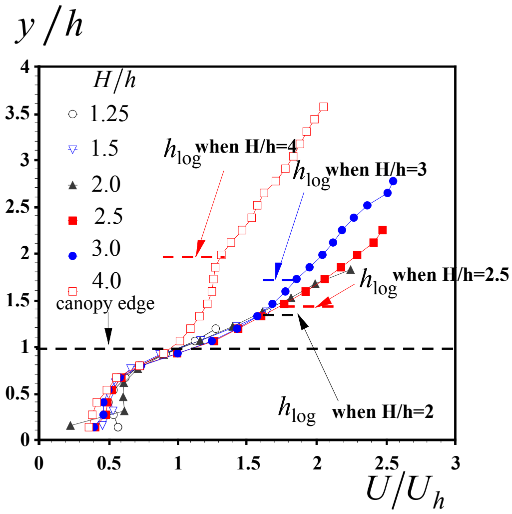

Fig. 3 Vertical profile of mean velocity

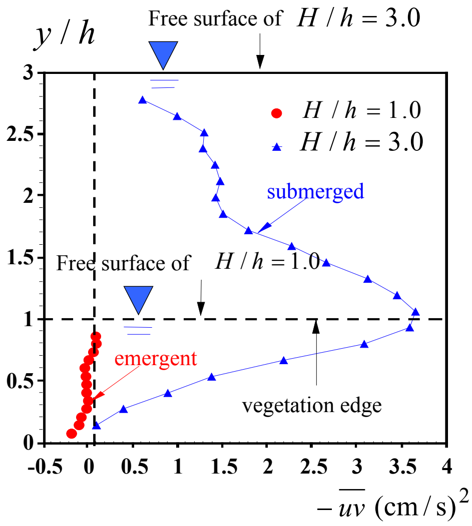

Fig. 4 Reynolds stress distribution for
the emergent and the submerged canopies

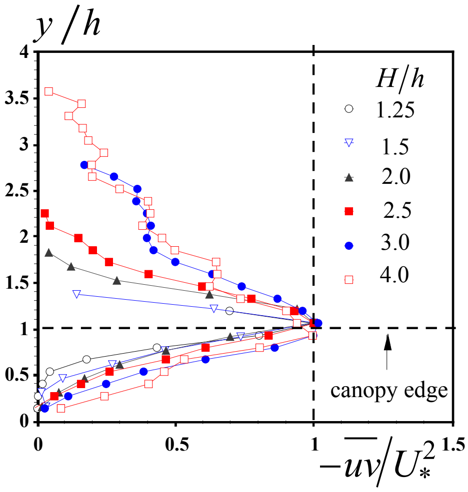

Fig. 5 Reynolds stress distribution

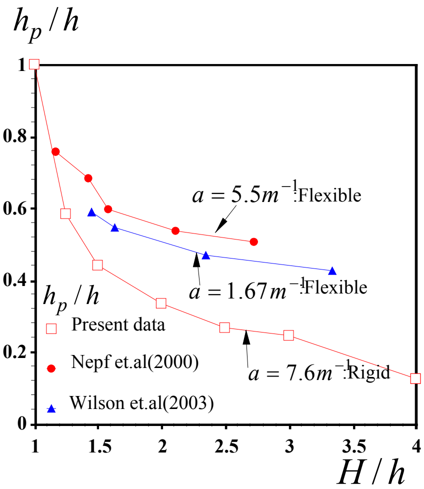

Fig. 6 Relation between penetration depth
and relative submergence

about 7m downstream from the channel entrance. The illuminated flow pictures were taken by a high-speed CMOS camera (1000×1000pixels) with 500Hz frame-rate and 60s sampling time. The instantaneous velocity components $(\tilde{u}, \tilde{v})$ on the *x-y* plane were calculated by the PIV algorithm for the whole depth region.

Table 1 shows the hydraulic condition. Seven kinds of experiments were conducted by changing the submergence depth, i.e., $H/h = 1.0, 1.25, 1.5, 2.0, 2.5, 3.0$, and 4.0. The bulk mean velocity was constant for all cases, i.e., $U_m = 10$ cm/s. $a = \sum_i A_i/(Sh)$ is the vegetation density. A_i is the frontal area of the vegetation models and *S* is the referred bed area.

3. RESULTS

3.1 Mean-Flow Profiles and Reynolds Stress Distribution

Fig.3 shows the vertical profiles of streamwise velocity $U(y)$ for all submergence depth. The velocity at the vegetation tip, $U_h \equiv U(h)$. An inflection point appears significantly

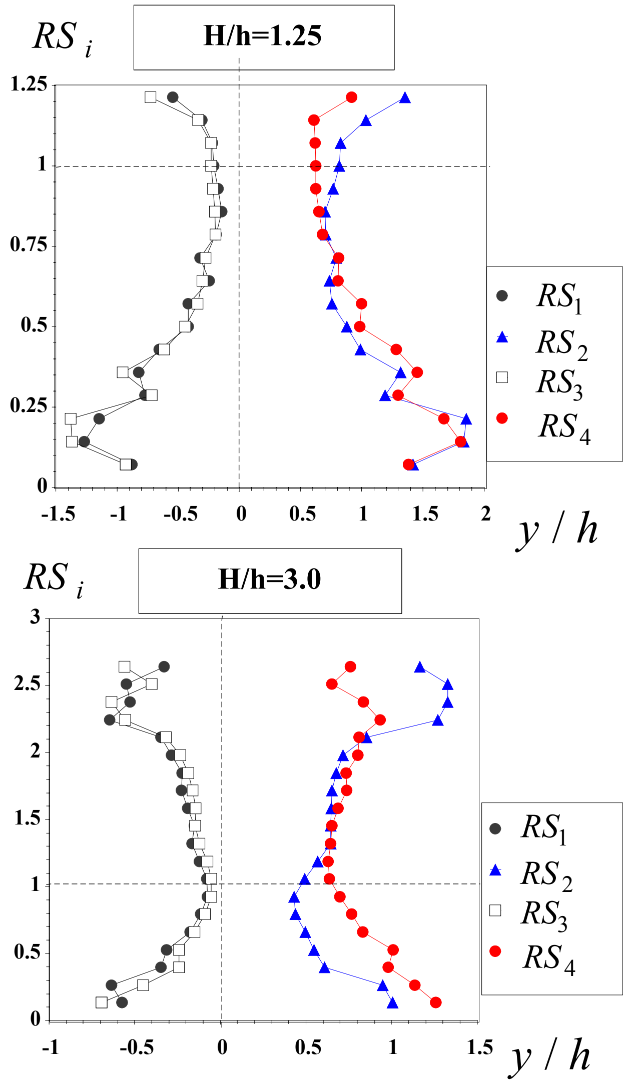

Fig. 7 Distribution of quadrant Reynolds stress

he values of U are normalized by the velocity near the canopy edge *y/h*=1. This is common tendency in all cases, irrespective of the submergence depth. In Fig.3, $h_{\log}$ is the lower limit position of "log-law zone", in which the mean velocity obeys log-law of roughness boundary layers.

Fig.4 shows the Reynolds stress distribution for emergent case (*H/h*=1.0) and submerged case (*H/h*=3.0). For submerged canopies, the Reynolds stress has a peak value near the vegetation edge, and decreases toward the free surface and the channel bed. In contrast, for emergent canopy, the values of $-\overline{uv}$ are very small in comparison with the submerged cases. This means that the vertical transport of momentum is negligibly small in emergent vegetation.

Fig.5 compares the vertical distribution of the normalized Reynolds stress $-\overline{uv}/U_*^2$ normalized by the friction velocity U_*. The values of U_* was evaluated from the peak value of $-\overline{uv}$. It was clearly found that the values of $-\overline{uv}$ increase with an increase of the submergence depth *H/h*. This reveals that the downward momentum transfer toward the within-canopy of $y < h$, is promoted more significantly as submergence depth increases.

Nepf & Vivoni (2000) defined a penetration height of momentum transfer, h_p, as the elevation of 10% of the maximum Reynolds stress. They evaluated the penetration of momentum into the canopy layer by h_p. Fig.6 shows the relations between h_p and *H/h*, which includes the data of Nepf & Vivoni (2000) & Wilson et al(2003). It is found that the value of h_p decreases rapidly, and becomes almost constant for *H/h*>2. This tendency agrees with the results of Nepf & Vivoni (2000) and Wilson et al(2003). The value of h_p is smaller in the present rigid vegetation than in the flexible ones in a wide range of the submergence depth. This may be because the oscillations of vegetation elements reduce the penetration of momentum into the canopy layer.

3.2 Quadrant Analysis

The quadrant analysis was conducted for the instantaneous Reynolds stress $-u(t)v(t)$. The quadrant Reynolds stress RS_i is defined as follows:

$$RS_i = \lim_{T \to \infty} \frac{1}{T} \int_0^T \left(\frac{uv}{\overline{uv}} \right) I_i dt \qquad (1)$$

If (u, v) exists in a quadrant i, then $I_i = 1$, and otherwise $I_i = 0$. Each quadrant of (u, v) corresponds to the following coherent events:

i=1 $(u > 0, v > 0)$: outward interaction
i=2 $(u < 0, v > 0)$: ejection
i=3 $(u > 0, v < 0)$: inward interaction
i=4 $(u < 0, v < 0)$: sweep

Fig.7 shows the vertical distributions of RS_i for *H/h*=1.25 and 3.0. For shallow submerged canopy flow (*H/h*=1.25), RS_4 is slightly larger than RS_2 within the canopy. For deep submergence depth (*H/h*=3.0), the sweep events are more predominant within the canopy. This suggests that the property of organized motion for deeper submergence resembles that of roughness open-channel flow more significantly than for shallow one. The latter rough wall was examined by Nezu & Nakagawa (1993).

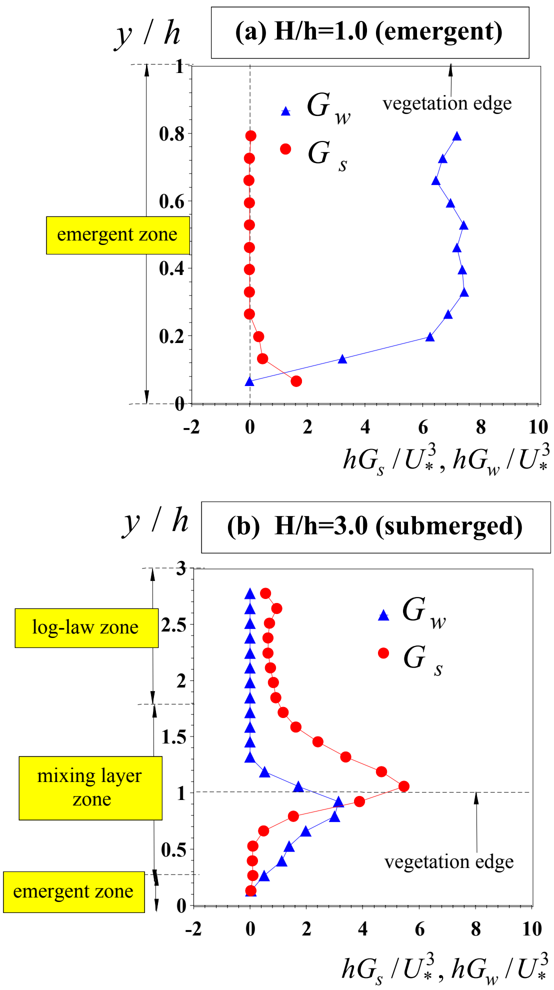

Fig. 8 Generation rate of turbulence energy

3.3 Generation Rate of Turbulence

Generation of turbulent energy is shown in Fig.8 for emergent canopy (*H/h*=1.0) and submerged canopy (*H/h*=3.0). The shear generation , G_s , is defined as:

$$G_s = -\overline{uv} \frac{\partial U}{\partial y} \qquad (2)$$

In contrast, the wake generation G_w due to vegetation wakes, was estimated as the work by the vegetation drag in the same way as Nepf & Vivoni (2000)

$$G_w = \frac{1}{2} C_D a U^3 \qquad (3)$$

in which C_D is the drag coefficient. The results are normalized by U_* and *h*. For the emergent canopy, the wake generation G_w is much larger than the shear generation G_s , as clearly seen in Fig.8 (a). This indicates that the small-scale wake turbulence is generated significantly behind vegetation stems in emergent vegetation.

In contrast, the shear generation G_s becomes more important source of turbulent energy in the mixing layer and log-law zones in the submerged flow (*H/h*=3.0), as seen in Fig.8 (b). G_w is comparable with G_s within the canopy.

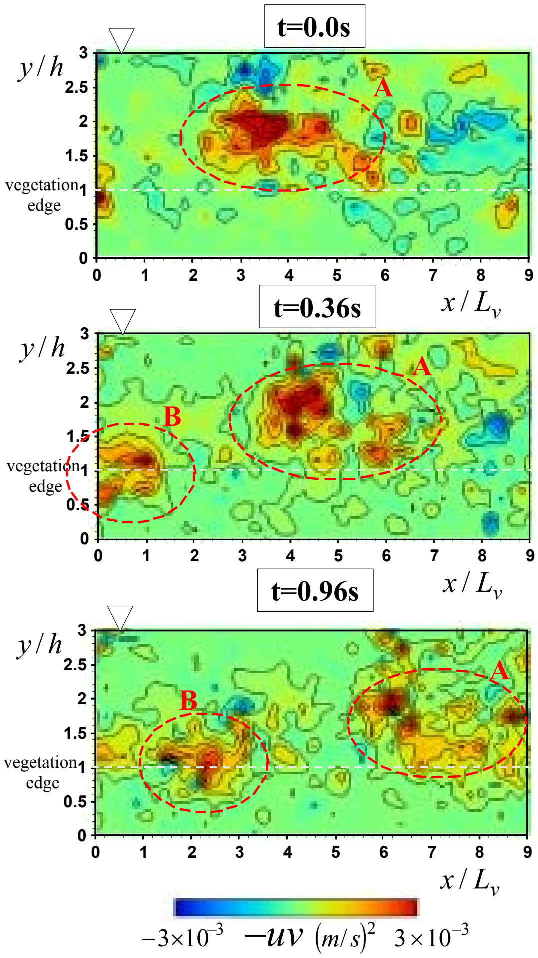

Fig. 9 Instantaneous Reynolds stress

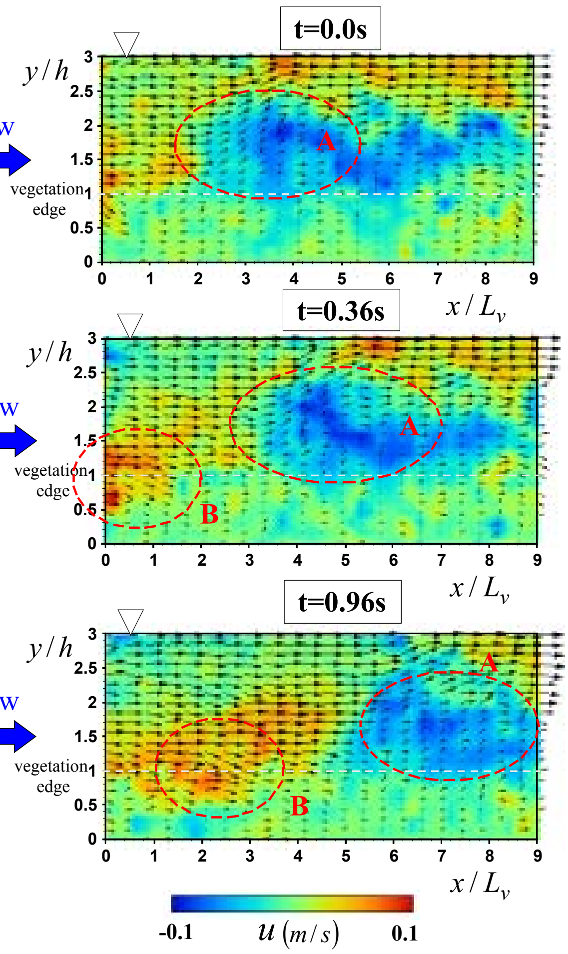

Fig. 10 Instantaneous velocity vectors (correspond to Fig.9)

3.4 Visualization of Coherent Motion

Fig.9 shows some examples of the contours of instantaneous Reynolds stress $-uv$ at t=0.0, 0.36 and 0.96 seconds for *H/h*=3.0. Fig.10 shows the time series of instantaneous velocity vectors, which corresponds to Fig.9. The contour of streamwise velocity fluctuations $u(x,y,t)$ is also depicted by rainbow in Fig.10.

In Fig.9, at $t=0$ s, some large positive regions of $-uv$ are observed locally above the vegetation edge and are indicated by dashed circle. It is found in Fig.10 that the ejection motion (dashed circle "A") appears over the vegetation edge, and that the low-speed fluid parcel is transported toward the free surface. At $t=0.36$ s, the sweep motion (dashed circle "B"), which is downward vectors of high-speed fluid parcel, is observed in the upstream side. At $t=0.96$ s, the ejections and sweeps are convected downstream. These results suggest that the local distributions of large Reynolds stress correspond well to these coherent structures. It was found from all digital pictures that the sweeps and ejections appear alternatively and periodically.

Fig.11 shows the relation between the submergence depth and the mean period of sweeps and ejections, T_S and T_E, in which T_M is the theoretical value of mean period in pure mixing layer proposed by Ho & Huerre (1984) in the following way.

$$T_M = \frac{\theta}{0.032\overline{U}} \tag{4}$$

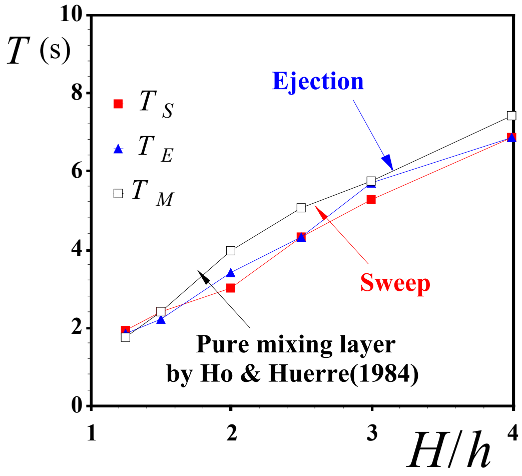

Fig. 11 Periodicity of coherent motions

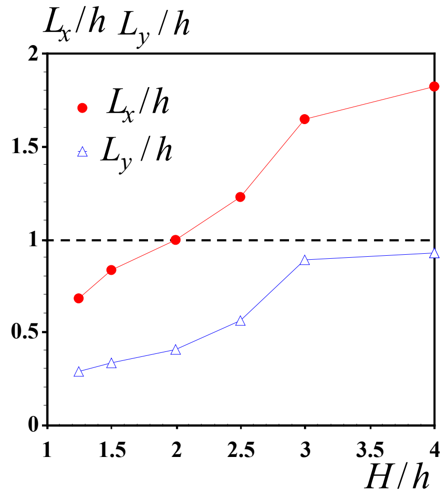

Fig. 12 Relation between length scale of coherent eddies and relative submergence

where, $\overline{U}=1/2(U_1+U_2)$, and θ is the momentum thickness. U_1 is the constant velocity of the low speed zone, and U_2 is the constant one of the high speed zone. Both of T_S and T_E are in good agreement with the theoretical value T_M for all submergence depth. This suggests that the coherent motion of the submerged canopy flows strongly resembles the mixing layer.

Same suggestions were also pointed out by Ikeda & Kanazawa(1996) and Ghisalberli & Nepf (2002) for aquatic canopy flows.

3.5 Length Scale of Coherent Eddy

A length scale of coherent eddy at the vegetation edge (*y/h*=1.0) can be evaluated from PIV data, as follows:

$$L_x \equiv \int_0^\infty \frac{\overline{u(x_0,y_0,t_0)u(x_0+x,y_0,t_0)}}{u'(x_0,y_0)u'(x_0+x,y_0)}dx \tag{5}$$

$$L_y \equiv \int_0^\infty \frac{\overline{u(x_0,y_0,t_0)u(x_0,y_0+y,t_0)}}{u'(x_0,y_0)u'(x_0,y_0+y)}dx \tag{6}$$

, in which L_x and L_y are the length scales in the streamwise and vertical directions. Fig.12 shows that L_x is larger than L_y for all cases of submergence depth, and it means that the oval vortices are generated near the vegetation edge, as has been seen in Fig.9. L_x and L_y increase with an increase of the submergence depth *H/h* and become almost constant for *H/h*>3.0. These suggest strongly that the development of coherent eddies is more confined by the existence of free surface in shallower submerged canopy flow.

4 CONCLUSIONS

In the present study, the effects of the submergence depth on turbulence structure were investigated in vegetated open-channel flows on the basis of PIV measurements. Consequently, mean-flow properties, turbulence structure and coherent motions were revealed and discussed. Main findings are as follows:

1) In deeply submerged flow, the vertical penetration of momentum into the canopy is promoted significantly, large-scale coherent motion.
2) On the basis of the quadrant analysis it was found that in deeply submerged flow the sweeps dominate the momentum transport in the same manner as roughness open-channel flow.
3) Sweeps and ejections appear alternatively periodically. The local distributions of large Reynolds stress are consistent well with these coherent structures.
4) The length scale of the coherent eddies was evaluated from the space correlations. It was found that the development of coherent eddies is more confined by the existence of free surface in shallower submerged canopy flows.

REFERENCES

1) Dwyer, M.J., Patton, E.G. and Shaw, R.H. (1997): Turbulence Kinetic Energy Budget from a Large-Eddy Simulation of Airflow above and within a Forest, *Boundary Layer Meteorology*, Vol. 84, pp.23-43.
2) Ghisalberti, M. and Nepf, H. (2002): Mixing layers and coherent structures in vegetated aquatic flows, *J. of Geophysical Res.,* Vol. 107, pp.3-1-3-11-
3) Ho, C.M. and Huerre, P. (1984): Perturbed free shear layers, Ann. *Rev. Fluid Mech*., Vol.16, pp.365-424.
4) Ikeda, S. and Kanazawa, M. (1996) : Three-dimensional organized vortices above flexible water plants, *J. of Hydraulic Eng.,* Vol. 122(11), pp.634-640.
5) Nepf, H. M. and Vivoni, E. R. (2000) : Flow Structure in Depth-limited, Vegetated Flow, *J. of Geophysical Res.,* Vol. 105, pp.28547-28557.
6) Nezu, I. and Nakagawa, H. (1993) : Turbulence in Open-Channel Flows, IAHR-Monograph, Balkema
7) Nezu, I., Sanjou, M. and Okamoto, T. (2006): Turbulent Structure and Dispersive Properties in Vegetated Canopy Open-channel Flows, *River Flow2006*, Lisbon, pp.583-592,.
8) Poggi, D., Porpotato, A. and Ridolfi, L. (2004). The effect of vegetation density on canopy sub-layer turbulence, *Boundary-Layer Meteorology,* Vol.111, pp.565-587.
9) Raupach, M. R., Coppin, P.A. and Legg, B.J. (1986): Experiments on scalar Dispersion within a Model Canopy, Part Ⅰ: Turbulence Structure, *Boundary-Layer Meteorology*., Vol.35, pp.21-52.
10) Wilson, C.A.M.E, Stoesser, T., Bates, P.D. and Batemann Pinzen, A. (2003) :Open Channel Flow through Different Forms of Submerged Flexible Vegetation, *J. of Hydraulic Engineering*, Vol. 129, pp.847-853